CHEMISTRY OF MATERIALS

pubs.acs.org/cm

Article

Rapid, Ambient Temperature Synthesis of Imine Covalent Organic Frameworks Catalyzed by Transition-Metal Nitrates

Dongyang Zhu, Zhuqing Zhang, Lawrence B. Alemany, Yilin Li, Njideka Nnorom, Morgan Barnes, Safiya Khalil, Muhammad M. Rahman, Pulickel M. Ajayan, and Rafael Verduzco*

Cite This: *Chem. Mater.* 2021, 33, 3394−3400

Read Online

ACCESS | Metrics & More | Article Recommendations | Supporting Information

ABSTRACT: Covalent organic frameworks (COFs) are crystalline, porous organic materials that are promising for applications including catalysis, energy storage, electronics, gas storage, water treatment, and drug delivery. Conventional solvothermal synthesis approaches require elevated temperatures, inert environments, and long reaction times. Herein, we show that transition-metal nitrates can catalyze the rapid synthesis of imine COFs under ambient conditions. We first tested a series of transition metals for the synthesis of a model COF and found that all transition-metal nitrates tested produced crystalline COF products even in the presence of oxygen. $Fe(NO_3)_3{\cdot}9H_2O$ was found to produce the most crystalline product, and crystalline COFs could be produced within 10 min by optimizing the catalyst loading. $Fe(NO_3)_3{\cdot}9H_2O$ was further tested as a catalyst for six different COF targets varying in linker lengths, substituents, and stabilities, and it effectively catalyzed the synthesis of all imine COFs tested. This catalyst was also successful in the synthesis of 2D imine COFs with different geometries, 3D COFs, and azine-linked COFs. This work demonstrates a simple, low-cost approach for the synthesis of imine COFs and will significantly lower the barrier for the development of imine COFs for applications.

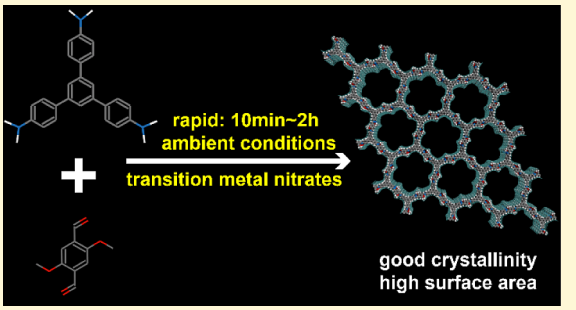

INTRODUCTION

Covalent organic frameworks (COFs) are crystalline and porous organic networks that are promising for applications including catalysis, energy storage, electronics, gas storage, water treatment, membrane separations, and drug delivery.[1−5] Imine COFs are of particular interest for applications because they exhibit excellent stability in water and various organic solvents.[5] However, imine COFs are typically synthesized in batch, high-temperature (120 °C) solvothermal or hydrothermal reactions that require 3 days or longer to achieve significant yields and good crystallinity.[3,5−7] Hence, simpler, lower-cost, and more rapid approaches to the synthesis of imine COFs are needed.

A number of studies have explored alternative, faster, and less energy-intensive approaches to the synthesis of imine COFs. Marder and co-workers developed an approach to produce imine COFs under solvothermal conditions within 4 h of using mild activation procedures to avoid pore collapse.[8] Wang and co-workers developed a general method to synthesize imine COFs in 160 s under electron beam irradiation.[9] Exposure to light,[10] reaction in a microwave,[11,12] and sonication[13] can also promote reversible reactions and tremendously decrease the required reaction time. In all of these examples, acetic acid was employed as the catalyst for imine COF synthesis.

Developing new catalysts for COF synthesis can further reduce the cost and time required to synthesize COFs, but very few catalysts for imine COF synthesis have been studied. A number of studies have utilized *p*-toluenesulfonic acid (PTSA) as a catalyst for COF synthesis,[14−16] with the advantage that it can be used to catalyze solid-state reactions. However, large amounts of PTSA are required, which may make it difficult or expensive to recycle the catalyst, and solid-state reactions come with additional challenges in terms of blending and processing the starting materials and final products. Metal triflates can catalyze the rapid synthesis of imine COFs,[17,18] but the best metal triflate catalyst for COFs relies on the expensive, rare-earth element scandium.[19,20]

Herein, we report that transition-metal nitrates catalyze the rapid synthesis of imine COFs at ambient temperatures with excellent yields. Transition-metal nitrates have been previously employed as catalysts for the synthesis of Schiff bases. Mobinikhaledi et al. used copper nitrate to synthesize Schiff bases rapidly and efficiently under ambient conditions.[21] In

Received: March 1, 2021
Revised: April 19, 2021
Published: April 29, 2021

another report, Mobinikhaledi et al. utilized a series of metal nitrates ranging from 5 to 20 mol % in the synthesis of Schiff bases containing the benzimidazole moiety at room temperature.[22] Through the optimization of different reaction conditions, they found that 5 mol % of $Ni(NO_3)_2{\cdot}6H_2O$ in methanol successfully generated Schiff bases with high yields and within just 20−30 min. Motivated by these findings, we explored the application of transition-metal nitrates in the synthesis of imine COFs. We tested six different transition-metal nitrates for use as catalysts in the synthesis of imine COFs under systematically varying reaction conditions and characterized the products through a combination of Fourier transform infrared (FT-IR) spectroscopy, powder X-ray diffractions (PXRD), nitrogen sorption analysis, and $^1H-^{13}C$ cross-polarization/magic-angle spinning (CPMAS) NMR. We found that catalytic amounts of transitional metal nitrates, in particular $Fe(NO_3)_3{\cdot}9H_2O$, effectively catalyzed Schiff base reactions and produced highly crystalline COFs at room temperature and for reaction times as short as 10 min. Furthermore, the reaction was not sensitive to oxygen. Transition-metal nitrates are low-cost, abundant catalysts, and this work demonstrates a simple and rapid approach to imine COFs. We expect that this will significantly lower the barriers for the synthesis and further development of COFs for various applications.

RESULTS AND DISCUSSION

We evaluated six different transition-metal nitrates for the synthesis of imine COFs: $Fe(NO_3)_3{\cdot}9H_2O$, $Ni(NO_3)_2{\cdot}6H_2O$, $Zn(NO_3)_2{\cdot}6H_2O$, $Mn(NO_3)_2{\cdot}6H_2O$, $Cu(NO_3)_2{\cdot}6H_2O$, and $Co(NO_3)_2{\cdot}6H_2O$. For simplicity, these catalysts will be referred to as M−NO, where M is the transition-metal (e.g., $Fe(NO_3)_3{\cdot}9H_2O$ will be referred to as Fe−NO). We initially evaluated these transition-metal catalysts for the synthesis of TAPB−OMePDA COF through the Schiff base polycondensation between 1,3,5-tris(4-aminophenyl)benzene (TAPB) and 2,5-dimethoxyterephthalaldehyde (OMePDA), as shown in Figure 1. We used this COF as a model system because it exhibits excellent crystallinity and porosity under a variety of synthesis and activation conditions, as demonstrated by Zhu et al.[23] and others.[8,24] To test each transition-metal catalyst, we dissolved a stoichiometric ratio of TAPB and OMePDA in 1,2-dichlorobenzene (DCB) and 1-butanol (1:1, v/v) and added 5 mol % catalyst relative to NH_2 functional groups. The reaction mixture was sonicated to ensure the full dissolution of the catalyst and then reacted at ambient temperatures, without any purging or heating of the reaction mixture. Upon sonication, insoluble powders were rapidly formed, and the mixture immediately turned cloudy and reddish. The reaction was allowed to proceed for 2 h before recovering the powders by filtration and washing with solvent and supercritical CO_2 ($ScCO_2$) prior to analysis.

FT-IR spectroscopy, $^1H-^{13}C$ CPMAS NMR spectroscopy, PXRD, and nitrogen sorption measurements revealed that the Schiff base reaction was successful and produced a crystalline and highly porous product. FT-IR (Figures S1 and S2) spectra revealed the formation of imine linkages with the appearance of a vibration peak at 1619 cm^{-1} and attenuation of the peak at 1685 cm^{-1}, corresponding to imine (C=N stretching) and aldehyde (C=O stretching) functional groups, respectively.[25,26] $^1H-^{13}C$ CPMAS NMR spectra provided strong evidence of extensive condensation of amino and aldehyde functional groups. Spectra obtained with a wide range of contact times

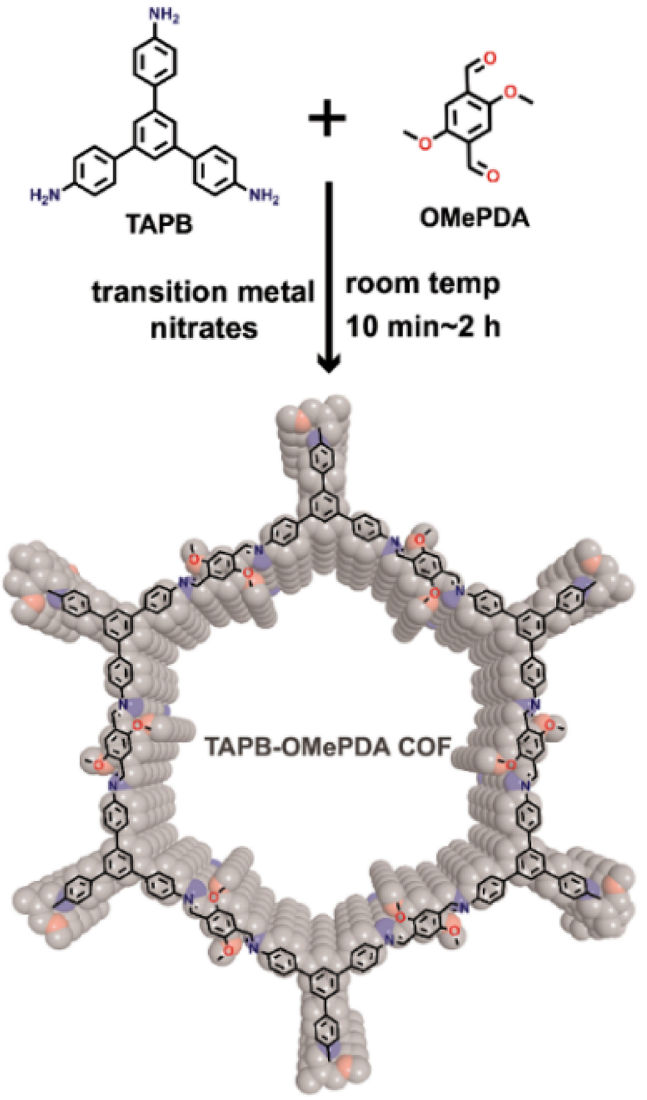

Figure 1. Rapid synthesis of TAPB−OMePDA COF catalyzed by transition-metal nitrates.

(Supporting Information) exhibited prominent, rapidly cross-polarizing signals at 155.8 and 150.4 ppm attributed to imino carbons in different environments but only extremely weak (or undetectable) aldehyde carbonyl signals from unreacted aldehyde groups on the edges of the COFs. PXRD (Figure 2) measurements showed that all solids possessed crystalline structures consistent with previous reports[23,24] and in agreement with simulated structures with AA stacking (Figure S3). The samples produced using the Fe−NO catalyst had the most prominent crystalline peaks, with a peak at $2\theta = 2.7°$, several orders of magnitude higher in intensity compared with other products. The product from the Fe−NO-catalyzed reaction also had the smallest full width at half-maximum values (Table S2). Nitrogen sorption isotherms of these samples and the corresponding Brunauer−Emmett−Teller (BET) surface areas (Figures S4 and S5) demonstrated that the products were highly porous and the Fe−NO produced samples with the highest porosities among all M−NO catalysts tested. The samples synthesized using Fe−NO and Ni−NO had surface areas of 1345 and 1214 $m^2\ g^{-1}$, respectively, which were higher than those synthesized using other metal nitrates. All samples had BET surface areas larger than 650 $m^2\ g^{-1}$, indicating that

https://doi.org/10.1021/acs.chemmater.1c00737
Chem. Mater. 2021, 33, 3394−3400

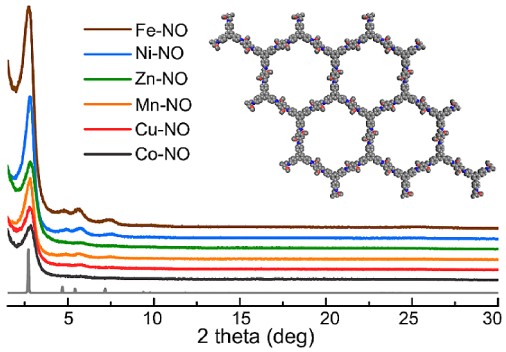

Figure 2. Experimental and simulated PXRD spectra for TAPB–OMePDA COFs synthesized with different transition-metal nitrates. The inset shows the illustration of the eclipsed structure.

all transition-metal nitrate catalysts successfully produced highly porous COFs. The pore size distributions of these samples were calculated using nonlocal density function theory (NLDFT) and are shown in Figure S4b. The samples catalyzed by Fe–NO had the narrowest pore size distribution centered around 2.7 nm, which matches that for prior reports of highly crystalline TAPB–OMePDA COF.[27] The samples synthesized using Ni–NO and Mn–NO catalysts also had relatively narrow pore size distributions, while the samples prepared using Zn–NO, Cu–NO, and Co–NO exhibited broader pore size distributions.

We also studied the effect of reaction time for different catalysts by analyzing the samples produced after 2 h and 3 days of total reaction time. The samples produced by Fe–NO and Ni–NO exhibited similar surface areas and crystallinities after 2 h and 3 days of reaction time, indicating that 2 h of reaction under ambient conditions was sufficient to produce highly crystalline products. After 3 days, crystallinity increased slightly, and Fe–NO and Ni–NO produced more crystalline samples compared to other metal nitrate catalysts, as evidenced by more prominent PXRD peaks (Figure S6), narrower pore size distributions (Figures S7 and S8), and higher surface areas (Figure S9 and S10). These results demonstrate that transition-metal nitrates, especially Fe–NO, are excellent catalysts for imine COF synthesis.

We next focused on the Fe–NO catalyst and optimized the catalyst loading. We chose six different catalyst loadings ranging from 1 to 10 mol % relative to NH_2 groups, which corresponded to less than 3.5 mol % relative to TAPB monomers. All other reaction conditions were kept the same, and the reactions were conducted at ambient temperatures and for 2 h reaction times. The samples produced with 10, 7, and 5 mol % Fe–NO showed the highest crystallinities and specific surface areas, as evidenced by PXRD and nitrogen sorption measurements, respectively (see Figures 3a,b and S11, and S12). These samples had surface areas of 1674, 1326, and 1345 $m^2\ g^{-1}$, respectively. They also exhibited narrower pore size distributions than other samples (Figure S13). To test whether residual iron remained in the final COF samples, we conducted high-resolution X-ray photoelectron spectroscopy (XPS, Figures S14 and S15) analysis for the sample synthesized using 10 mol % Fe–NO. We detected only a weak Fe $2p_{3/2}$ signal in the high-resolution spectra, corresponding to approximately 0.02 atom % or 0.1 wt % of the total including C 1s, N 1s, and O 1s signals. Additionally, no Fe–N coordination peak was observed in the N 1s spectrum,

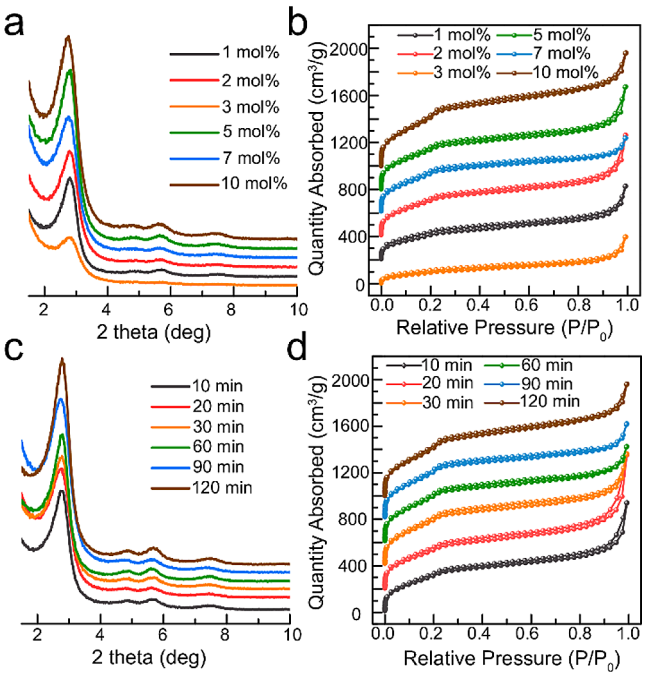

Figure 3. (a) PXRD patterns and (b) nitrogen sorption isotherms for TAPB–OMePDA COFs synthesized using different amounts of Fe–NO for 2 h; the isotherms are vertically offset by 200 (1 mol %), 400 (2 mol %), 600 (7 mol %), 800 (5 mol %), and 1000 (10 mol %) $cm^3\ g^{-1}$. (c) PXRD patterns and (d) nitrogen sorption isotherms for TAPB–OMePDA COFs synthesized using 10 mol % Fe–NO for different times ranging from 10 min to 2 h. The isotherms are vertically offset by 200 (20 min), 400 (30 min), 600 (60 min), 800 (90 min), and 1000 (120 min) $cm^3\ g^{-1}$.

indicating that the imine bond did not coordinate with iron.[28−30] No metallic iron (Fe^0) peak[31] was found in the iron element spectra, indicating that Fe^{3+} was not reduced into metallic iron nanoparticles by 1-butanol during the reaction process. Additionally, inductively coupled plasma–optical emission spectrometry (ICP-OES) indicated that the iron content was 0.13 wt %, similar to the value measured via XPS.

Next, we explored the effect of reaction time by varying the total reaction time from 10 min to 2 h using 10 mol % Fe–NO as the catalyst and keeping all other reaction conditions unchanged. The crystallinity and porosity increased with time, as evidenced by PXRD (Figure 3c) and nitrogen sorption analysis (Figures 3d and S16–S18). However, after 10 min of reaction time, all samples had very high surface areas of 1233 $m^2\ g^{-1}$ or greater, ranging from 1233 $m^2\ g^{-1}$ for 10 min reaction time to 1674 $m^2\ g^{-1}$ for 120 min (Figure S16). These results indicate that the highly crystalline COF formed within 10 min of reaction time. The surface area values were comparable to other studies reporting the synthesis of the TAPB–OMePDA COF using acetic acid catalyst at 120 °C for 3 days[32−34] and only slightly lower than that reported by Marder and co-workers using solvothermal conditions along with nitrogen flow activation.[8] All samples showed narrow pore size distributions (Figure S18), further demonstrating that 10 mol % Fe–NO successfully catalyzed the synthesis of the highly crystalline TAPB–OMePDA COF with regular porosity.

To test the broader effectiveness of transition-metal nitrates as catalysts for imine COF synthesis, we used the Fe–NO catalyst and targeted a series of COFs varying in structure and

https://doi.org/10.1021/acs.chemmater.1c00737
Chem. Mater. 2021, 33, 3394−3400

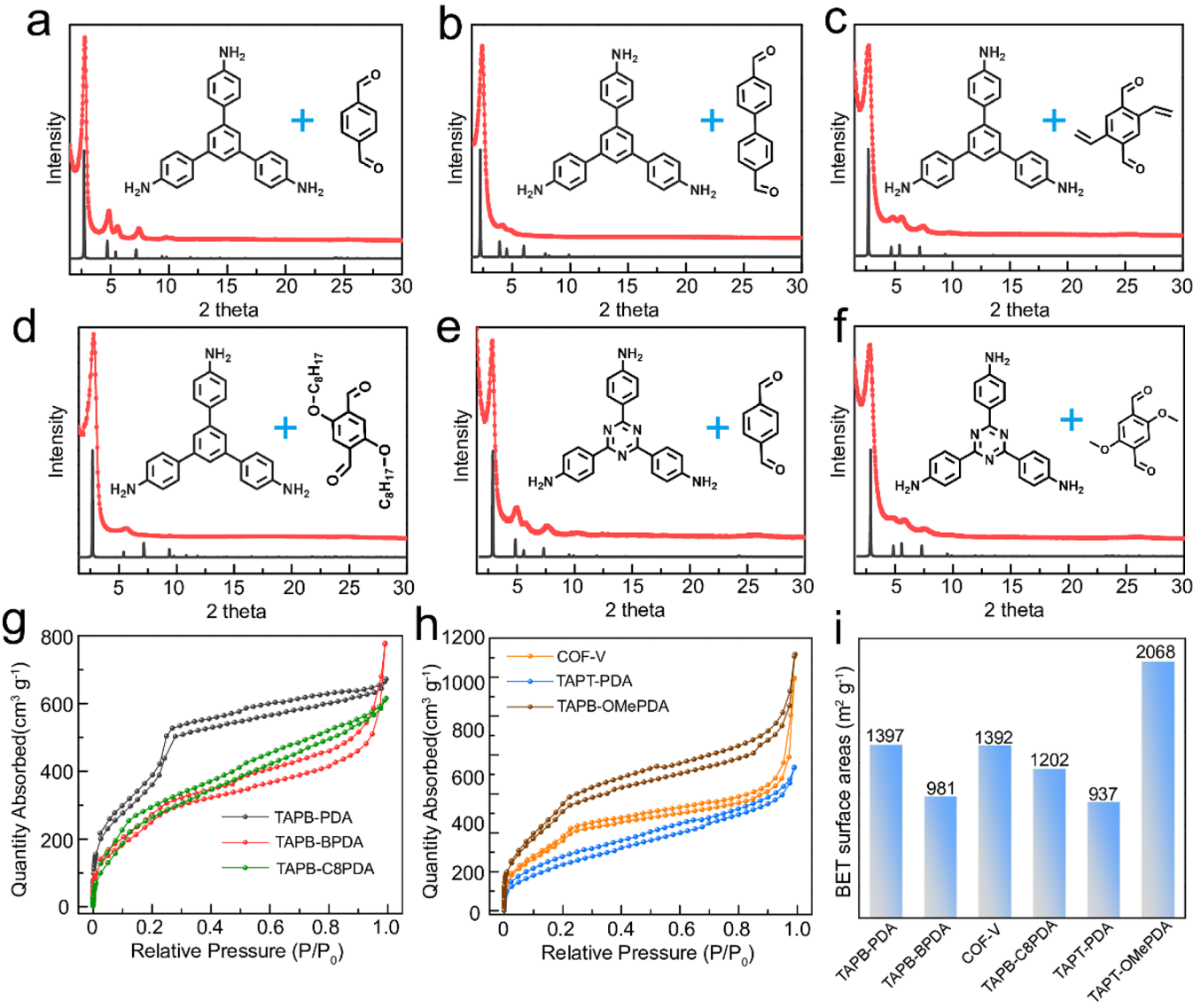

Figure 4. PXRD patterns for (a) TAPB−PDA COF produced by the reaction between TAPB and PDA, (b) TAPB−BPDA COF produced by the reaction between TAPB and BPDA, (c) COF−V produced by the reaction between TAPB and vinyl-PDA, (d) TAPB−C8PDA COF produced by the reaction between TAPB and C8PDA, (e) TAPT−PDA COF produced by the reaction between 2,4,6-tris(4-aminophenyl)-1,3,5-triazine (TAPT) and PDA, (f) TAPT−OMePDA COF produced by the reaction between TAPT and OMePDA, (g, h) nitrogen sorption isotherms, and (i) BET surface areas.

stability (Figure 4). All the COFs selected as targets have been previously synthesized using acetic acid as a catalyst,[23,34−38] with the exception of TAPB−4,4′-biphenyldicarboxaldehyde (BPDA) COF, which has only been previously synthesized using scandium(III) triflate ($Sc(OTf)_3$) catalyst.[17] We altered the linker length (i.e., BPDA) and the substituents of aldehyde monomers (i.e., 2,5-divinylterephthalaldehyde (vinyl-PDA), 2,5-bis(octyloxy)terephthalaldehyde (C8PDA)) to test the functional group tolerance of the Fe−NO catalyst. We also targeted COFs of different structural stabilities. Prior work has shown that some COFs are more robust under different activation processes and maintain excellent crystallinity and surface area, while other COFs are fragile and lose crystallinity when activated using polar solvents.[8,23,24] We selected both fragile (TAPB−terephthalaldehyde (PDA), TAPB−BPDA, 2,4,6-tris(4-aminophenyl)-1,3,5-triazine (TAPT)−PDA) and robust COFs (COF−V, TAPB−C8PDA, TAPT−OMePDA) for synthesis using the Fe−NO catalyst. All reactions were conducted using 10 mol % Fe−NO for 2 h, and the samples were thoroughly washed and dried using $ScCO_2$ prior to analysis. FT-IR spectra of the final solid products (Figures S19−S24) confirmed the successful imine polycondensation for all samples tested and were consistent with previous reports.[17,23,34,35,39−41] All samples exhibited excellent crystallinity, as evidenced by prominent peaks in the PXRD spectra (Figure 4a−f), which were consistent with both previous studies and simulated eclipsed, layered structures (Figures 4a−f and S25−S30). We further calculated their pore size distributions from nitrogen sorption tests using the NLDFT method and found that all samples possessed narrow pore size distributions (Figure S31). The BET surface areas for TAPB−PDA COF, TAPB−BPDA COF, COF−V, TAPB−C8PDA COF, TAPT−PDA COF, and TAPT−OMePDA COF were 1397, 981, 1392, 1202, 937, and 2068 $m^2\ g^{-1}$, respectively (Figure 4i, S32). Notably, Fe−NO was successful in catalyzing the synthesis of highly crystalline TAPB−BPDA COFs, which

https://doi.org/10.1021/acs.chemmater.1c00737
Chem. Mater. 2021, 33, 3394−3400

has not previously been synthesized using acetic acid catalyst. We also could not produce crystalline TAPT−PDA COFs using solvothermal methods with acetic acid catalyst and various solution conditions (see the Supporting Information). This is consistent with two previous reports that reported TAPT−PDA COFs with limited crystallinity and low porosity.[39,40] However, highly crystalline powders could be synthesized within 2 h utilizing the Fe−NO catalyst. To compare the quality of COFs that we synthesized with those from other reports, we compared the BET surface areas produced using Fe−NO with the highest values from prior reports, as shown in Table S3. COF−V, TAPB−C8PDA COF, TAPT−PDA COF, and TAPT−OMePDA COF synthesized using our approach showed higher BET surface areas than the highest records from previous reports.[34−38] These experiments demonstrated the general effectiveness of the Fe−NO catalyst for imine COF synthesis, and it is likely that COFs with even higher quality can be produced with additional optimization.

We further tested the use of transition-metal nitrates in the synthesis of 2D imine COFs with different geometries, 3D imine COFs, and different COF chemistries. In particular, we targeted the synthesis of 2D imine COFs with 3 + 3 (Scheme S7) and 4 + 2 (Scheme S8) node-linker functionalities, 3D imine COFs (Table S4 and S5), azine-linked COFs (Scheme S9), β-ketoenamine COFs (Table S7), and hydrazone COFs (Table S8). Fe−NO (10 mol %, 2 h) successfully catalyzed the synthesis of a highly crystalline 3 + 3 2D imine COF through the condensation of TAPT and 1,3,5-tris(4-formylphenyl)-benzene (TFPB) (Figures S33 and S34). The resulting COF was highly crystalline with a high BET surface area (838 m^2 g^{-1}; Figure S33). Due to the poor solubility of 1,3,6,8-tetrakis(4-aminophenyl)pyrene (Py), we were unable to produce the crystalline Py−1P imine COF using Py and PDA through a 4 + 2 construction strategy at room temperature. In the synthesis of 3D imine COFs, we found that Cu−NO effectively catalyzed the synthesis of COF-320 and COF-300 (Tables S4 and S5 and Figures S35−S38). Both crystalline COF-320 and COF-300 were produced within 4 h using 10 mol % Cu−NO at room temperature. Partially crystalline COF-320 and COF-300 could also be produced using Ni−NO and Zn−NO catalysts. Additionally, 10 mol% Cu−NO also rapidly catalyzed the synthesis of azine-linked COF (ACOF-1, Scheme S9, Figures S39 and S40) at room temperature. However, no crystallinity of 3D COFs and azine-linked ACOF-1 were observed for samples synthesized using 6 M acetic acid and $Sc(OTf)_3$ under the same conditions. We also explored the synthesis of β-ketoenamine and hydrazone COFs (see details in the Supporting Information, Tables S7 and S8, and Figure S41). Possibly because of the poor solubility of 2,4,6-triformylphloroglucinol (TFP), we could only produce β-ketoenamine COFs with limited crystallinity using various transition-metal nitrates and 6 h reaction time at room temperature. An improvement in crystallinity was observed for 6 h reaction time at 120 °C (see Table S7). Crystalline hydrazone COFs could not be synthesized within 2 h at room temperature using metal nitrates or solvothermal conditions with acetic acid or $Sc(OTf)_3$ (see Table S8 and details in Supporting Information). This may be due to the low reactivity and poor solubility of a hydrazide monomer at room temperature. In general, the number and variety of hydrazone COFs reported are much more limited than imine COFs.

A detailed study of the catalytic mechanism of the Schiff base reaction by transition-metal nitrates is outside the scope of this work, but it is likely related to the Brønsted acid nature of the transition metals in water or alcohol.[42,43] Hydrated metal ions can form complex ions with water or 1-butanol, resulting in solution acidity and increasing the rate of the Schiff base reaction. Future work will focus on understanding how different metal ions influence the Schiff base reaction.

Our results demonstrate that transition-metal nitrates are effective catalysts for the synthesis of imine COFs. Unlike the conventional solvothermal methods and a recent report using electron irradiation to rapidly synthesize COFs,[9] reactions catalyzed by metal nitrates were effective at ambient temperatures and without the need for purging the reaction to eliminate oxygen. Compared to $Sc(OTf)_3$ catalyst,[17,18] metal nitrates are of low cost and abundant. Additionally, the excellent solubility of metal nitrates in various alcohols and acetonitrile make them promising for the interfacial synthesis of COF films. We are actively pursuing the use of transition-metal nitrates to synthesize imine COF films and membranes.

CONCLUSION

In conclusion, we demonstrated that transition-metal nitrates, particularly $Fe(NO_3)_3{\cdot}9H_2O$, are excellent catalysts for imine COF synthesis. We were able to synthesize TAPB−OMePDA COFs with high crystallinity and surface areas within 10 min, and we produced a series of crystalline imine COFs rapidly at ambient temperatures. We expect that this will significantly lower the barriers for the synthesis and further development of COFs for various applications.

EXPERIMENTAL SECTION

Chemicals. All chemicals were purchased from commercial sources and used without further purification. TAPB was purchased from TCI America. PDA, OMePDA, benzene-1,4-diamine, hydrazine monohydrate ($NH_2NH_2{\cdot}H_2O$), $Sc(OTf)_3$, anhydrous 1-butanol, 1,4-DCB, dioxane, and mesitylene were purchased from Sigma-Aldrich. BPDA and TAPT were purchased from AmBeed. C8PDA, vinyl-PDA, benzene-1,3,5-tricarbaldehyde, TFPB, Py, tetrakis(4-aminophenyl)-methane, TFP, and 2,5-diethoxyterephthalohydrazide were purchased from the Jilin Chinese Academy of Sciences—Yanshen Technology Co., Ltd. All other solvents used in this work were purchased from Fisher Scientific.

Instrumentations and Characterizations. PXRD data were collected on a Rigaku SmartLab XRD with 2θ ranging from 1° to 30° with 0.02° increment in a continuous mode. Powder samples without prior grinding were directly placed on zero background sample holders and leveled flat using a glass microscope slide. FT-IR spectra were measured using a Thermo Nicolet iS10 FT-IR spectrometer with a diamond ATR attachment and were uncorrected. The testing range was set from 4000 to 500 cm^{-1}. Nitrogen sorption measurements were conducted on an Autosorb-iQ-MP/Kr BET Surface Analyzer (Quantachrome Instruments). The samples were dried using $ScCO_2$ and further degassed to remove residual CO_2 at 80 °C under vacuum. All samples were tested directly without grinding. BET surface areas were calculated using BET adsorption models included in the instrument software (ASiQwin Version 5.2). XPS spectra were collected using a PHI Quantera SXM scanning X-ray microprobe with a base pressure of 5×10^{-9} Torr. Survey spectra were collected using 0.5 eV step sizes with a pass energy of 140 eV. Elemental spectra were recorded using 0.1 eV step sizes with a pass energy of 26 eV. ICP-OES was conducted using an Agilent 725 ICP-OES. The as-synthesized COF powders were fully digested using metal-free concentrated nitric acid at 80 °C and then diluted for testing. The percentage of residual iron in the COF matrix was 0.13 wt %. $^1H-^{13}C$ CPMAS spectra were obtained on a Bruker 4.7 T NMR spectrometer previously described in detail[44] and with the data acquisition and processing parameters previously described[44] except for the number of scans (5200) and the

https://doi.org/10.1021/acs.chemmater.1c00737
Chem. Mater. 2021, 33, 3394−3400

amount of line broadening used in processing the FID (50 Hz). There was enough TAPB−OMePDA COF to fill only about two-thirds of a standard 4 mm rotor. Just enough space remained to add a silicon nitride upper plug to confine the material closer to the center of the rotor. With the sample spinning at 7.6 kHz, 15 spectra with contact times t_{cp} ranging from 0.1 to 5.5 ms were obtained for each sample to study the relative rates of cross-polarization for the different carbon environments, with a 5 min waiting period preceding each experiment to ensure complete relaxation. In addition, at the contact time that appeared optimal for maximizing the intensity of the quaternary carbon signals (3.0 ms), dipolar dephasing experiments were performed with 50 and 80 μs dephasing intervals to provide additional evidence for differentiating proton-bearing from quaternary carbons.

$ScCO_2$ Drying. $ScCO_2$ drying was conducted on a Leica EM CPD300 Automated Critical Point Dryer. All products were separated and washed thoroughly using THF/water, acetone, and pure ethanol. Washing with a large excess of water is important to remove any of the water-soluble metal nitrate catalysts. Wetted COF powders were loaded in tea bags (ETS Drawstring Tea Filters, sold by English Tea Store, Amazon.com), immersed in pure ethanol, and then placed in the dryer chambers with the addition of an appropriate amount of pure ethanol. The program was totally automated. The chamber was first cooled down to 14 °C, and then $ScCO_2$ slowly flow into the chamber and exchanged for 14 cycles to replace the last-cycle solvents. Later, the chamber was warmed to 35 °C at a medium rate, and finally, the CO_2 gas was released in a fast speed.

■ ASSOCIATED CONTENT

Supporting Information

The Supporting Information is available free of charge at https://pubs.acs.org/doi/10.1021/acs.chemmater.1c00737.

Materials, detailed synthesis procedures, summary of BET surface areas for different COFs from previous report, COF AA stacking structures, and additional characterization analysis (PDF)

■ AUTHOR INFORMATION

Corresponding Author

Rafael Verduzco − *Department of Chemical and Biomolecular Engineering, Rice University, Houston, Texas 77005, United States; Department of Materials Science and NanoEngineering, Rice University, Houston, Texas 77005, United States;* orcid.org/0000-0002-3649-3455; Email: rafaelv@rice.edu

Authors

Dongyang Zhu − *Department of Chemical and Biomolecular Engineering, Rice University, Houston, Texas 77005, United States;* orcid.org/0000-0002-3413-5419

Zhuqing Zhang − *Department of Chemical and Biomolecular Engineering, Rice University, Houston, Texas 77005, United States*

Lawrence B. Alemany − *Shared Equipment Authority and Department of Chemistry, Rice University, Houston, Texas 77005, United States;* orcid.org/0000-0001-7451-1020

Yilin Li − *Department of Chemical and Biomolecular Engineering, Rice University, Houston, Texas 77005, United States;* orcid.org/0000-0001-9408-6738

Njideka Nnorom − *Department of Chemical and Biomolecular Engineering, Rice University, Houston, Texas 77005, United States*

Morgan Barnes − *Department of Materials Science and NanoEngineering, Rice University, Houston, Texas 77005, United States*

Safiya Khalil − *Department of Chemical and Biomolecular Engineering, Rice University, Houston, Texas 77005, United States*

Muhammad M. Rahman − *Department of Materials Science and NanoEngineering, Rice University, Houston, Texas 77005, United States;* orcid.org/0000-0003-1374-0561

Pulickel M. Ajayan − *Department of Materials Science and NanoEngineering, Rice University, Houston, Texas 77005, United States;* orcid.org/0000-0001-8323-7860

Complete contact information is available at: https://pubs.acs.org/10.1021/acs.chemmater.1c00737

Notes

The authors declare no competing financial interest.

■ ACKNOWLEDGMENTS

The authors acknowledge financial support from the Army Research Laboratory (W911NF-18-2-0062) and the Welch Foundation for Chemical Research (C-1888). The authors also acknowledge the Shared Equipment Authority at Rice University for access and utilization of characterization instruments.

■ REFERENCES

(1) Ding, S.-Y.; Wang, W. Covalent Organic Frameworks (COFs): From Design to Applications. *Chem. Soc. Rev.* **2013**, *42*, 548−568.

(2) Feng, X.; Ding, X.; Jiang, D. Covalent Organic Frameworks. *Chem. Soc. Rev.* **2012**, *41*, 6010−6022.

(3) Kandambeth, S.; Dey, K.; Banerjee, R. Covalent Organic Frameworks: Chemistry beyond the Structure. *J. Am. Chem. Soc.* **2019**, *141*, 1807−1822.

(4) Huang, N.; Wang, P.; Jiang, D. Covalent Organic Frameworks: A Materials Platform for Structural and Functional Designs. *Nat. Rev. Mater.* **2016**, *1*, 1−19.

(5) Lohse, M. S.; Bein, T. Covalent Organic Frameworks: Structures, Synthesis, and Applications. *Adv. Funct. Mater.* **2018**, *28*, No. 1705553.

(6) Geng, K.; He, T.; Liu, R.; Dalapati, S.; Tan, K. T.; Li, Z.; Tao, S.; Gong, Y.; Jiang, Q.; Jiang, D. Covalent Organic Frameworks: Design, Synthesis, and Functions. *Chem. Rev.* **2020**, *120*, 8814−8933.

(7) Li, Y.; Chen, W.; Xing, G.; Jiang, D.; Chen, L. New Synthetic Strategies toward Covalent Organic Frameworks. *Chem. Soc. Rev.* **2020**, *49*, 2852−2868.

(8) Feriante, C. H.; Jhulki, S.; Evans, A. M.; Dasari, R. R.; Slicker, K.; Dichtel, W. R.; Marder, S. R. Rapid Synthesis of High Surface Area Imine-Linked 2D Covalent Organic Frameworks by Avoiding Pore Collapse During Isolation. *Adv. Mater.* **2020**, *32*, No. 1905776.

(9) Zhang, M.; Chen, J.; Zhang, S.; Zhou, X.; He, L.; Sheridan, M. V.; Yuan, M.; Zhang, M.; Chen, L.; Dai, X.; Ma, F.; Wang, J.; Hu, J.; Wu, G.; Kong, X.; Zhou, R.; Albrecht-Schmitt, T. E.; Chai, Z.; Wang, S. Electron Beam Irradiation as a General Approach for the Rapid Synthesis of Covalent Organic Frameworks under Ambient Conditions. *J. Am. Chem. Soc.* **2020**, *142*, 9169−9174.

(10) Kim, S.; Choi, H. C. Light-Promoted Synthesis of Highly-Conjugated Crystalline Covalent Organic Framework. *Commun. Chem.* **2019**, *2*, 1−8.

(11) Campbell, N. L.; Clowes, R.; Ritchie, L. K.; Cooper, A. I. Rapid Microwave Synthesis and Purification of Porous Covalent Organic Frameworks. *Chem. Mater.* **2009**, *21*, 204−206.

(12) Wei, H.; Chai, S.; Hu, N.; Yang, Z.; Wei, L.; Wang, L. The Microwave-Assisted Solvothermal Synthesis of a Crystalline Two-Dimensional Covalent Organic Framework with High CO_2 Capacity. *Chem. Commun.* **2015**, *51*, 12178−12181.

(13) Yang, S.-T.; Kim, J.; Cho, H.-Y.; Kim, S.; Ahn, W.-S. Facile Synthesis of Covalent Organic Frameworks COF-1 and COF-5 by Sonochemical Method. *RSC Adv.* **2012**, *2*, 10179−10181.

(14) Biswal, B. P.; Chandra, S.; Kandambeth, S.; Lukose, B.; Heine, T.; Banerjee, R. Mechanochemical Synthesis of Chemically Stable Isoreticular Covalent Organic Frameworks. *J. Am. Chem. Soc.* **2013**, *135*, 5328−5331.
(15) Shinde, D. B.; Aiyappa, H. B.; Bhadra, M.; Biswal, B. P.; Wadge, P.; Kandambeth, S.; Garai, B.; Kundu, T.; Kurungot, S.; Banerjee, R. A Mechanochemically Synthesized Covalent Organic Framework as a Proton-Conducting Solid Electrolyte. *J. Mater. Chem. A* **2016**, *4*, 2682−2690.
(16) Karak, S.; Kandambeth, S.; Biswal, B. P.; Sasmal, H. S.; Kumar, S.; Pachfule, P.; Banerjee, R. Constructing Ultraporous Covalent Organic Frameworks in Seconds via an Organic Terracotta Process. *J. Am. Chem. Soc.* **2017**, *139*, 1856−1862.
(17) Matsumoto, M.; Dasari, R. R.; Ji, W.; Feriante, C. H.; Parker, T. C.; Marder, S. R.; Dichtel, W. R. Rapid, Low Temperature Formation of Imine-Linked Covalent Organic Frameworks Catalyzed by Metal Triflates. *J. Am. Chem. Soc.* **2017**, *139*, 4999−5002.
(18) Matsumoto, M.; Valentino, L.; Stiehl, G. M.; Balch, H. B.; Corcos, A. R.; Wang, F.; Ralph, D. C.; Mariñas, B. J.; Dichtel, W. R. Lewis-Acid-Catalyzed Interfacial Polymerization of Covalent Organic Framework Films. *Chem.* **2018**, *4*, 308−317.
(19) Emsley, J. Unsporting Scandium. *Nat. Chem.* **2014**, *6*, 1025−1025.
(20) Røyset, J.; Ryum, N. Scandium in Aluminium Alloys. *Int. Mater. Rev.* **2005**, *50*, 19−44.
(21) Mobinikhaledi, A.; Steel, P. J.; Polson, M. Rapid and Efficient Synthesis of Schiff Bases Catalyzed by Copper Nitrate. *Synth. React. Inorg. Met.-Org. Nano-Met. Chem.* **2009**, *39*, 189−192.
(22) Mobinikhaledi, A.; Foroughifar, N.; Kalhor, M. An Efficient Synthesis of Schiff Bases Containing Benzimidazole Moiety Catalyzed by Transition Metal Nitrates. *Turk. J. Chem.* **2010**, *34*, 367−374.
(23) Zhu, D.; Verduzco, R. Ultralow Surface Tension Solvents Enable Facile COF Activation with Reduced Pore Collapse. *ACS Appl. Mater. Interfaces* **2020**, *12*, 33121−33127.
(24) Sick, T.; Rotter, J. M.; Reuter, S.; Kandambeth, S.; Bach, N. N.; Döblinger, M.; Merz, J.; Clark, T.; Marder, T. B.; Bein, T.; Medina, D. D. Switching on and off Interlayer Correlations and Porosity in 2D Covalent Organic Frameworks. *J. Am. Chem. Soc.* **2019**, *141*, 12570−12581.
(25) Smith, B. J.; Overholts, A. C.; Hwang, N.; Dichtel, W. R. Insight into the Crystallization of Amorphous Imine-Linked Polymer Networks to 2D Covalent Organic Frameworks. *Chem. Commun.* **2016**, *52*, 3690−3693.
(26) Zhu, D.; Alemany, L. B.; Guo, W.; Verduzco, R. Enhancement of Crystallinity of Imine-Linked Covalent Organic Frameworks via Aldehyde Modulators. *Polym. Chem.* **2020**, *11*, 4464−4468.
(27) Du, Y.-R.; Xu, B.-H.; Pan, J.-S.; Wu, Y.-W.; Peng, X.-M.; Wang, Y.-F.; Zhang, S.-J. Confinement of Brønsted Acidic Ionic Liquids into Covalent Organic Frameworks as a Catalyst for Dehydrative Formation of Isosorbide from Sorbitol. *Green Chem.* **2019**, *21*, 4792−4799.
(28) Jiao, L.; Wan, G.; Zhang, R.; Zhou, H.; Yu, S.-H.; Jiang, H.-L. From Metal−Organic Frameworks to Single-Atom Fe Implanted N-Doped Porous Carbons: Efficient Oxygen Reduction in Both Alkaline and Acidic Media. *Angew. Chem., Int. Ed.* **2018**, *57*, 8525−8529.
(29) Can, F.; Demirci, O. C.; Dumoulin, F.; Erhan, E.; Arslan, L. C.; Ergenekon, P. Iron Porphyrin-Modified PVDF Membrane as a Biomimetic Material and Its Effectiveness on Nitric Oxide Binding. *Appl. Surf. Sci.* **2017**, *420*, 625−630.
(30) Yu, Y.; Xiao, D.; Ma, J.; Chen, C.; Li, K.; Ma, J.; Liao, Y.; Zheng, L.; Zuo, X. The Self-Template Synthesis of Highly Efficient Hollow Structure Fe/N/C Electrocatalysts with Fe−N Coordination for the Oxygen Reduction Reaction. *RSC Adv.* **2018**, *8*, 24509−24516.
(31) Cano, A.; Lartundo-Rojas, L.; Shchukarev, A.; Reguera, E. Contribution to the Coordination Chemistry of Transition Metal Nitroprussides: A Cryo-XPS Study. *New J. Chem.* **2019**, *43*, 4835−4848.
(32) Li, X.; Zhang, C.; Cai, S.; Lei, X.; Altoe, V.; Hong, F.; Urban, J. J.; Ciston, J.; Chan, E. M.; Liu, Y. Facile Transformation of Imine Covalent Organic Frameworks into Ultrastable Crystalline Porous Aromatic Frameworks. *Nat. Commun.* **2018**, *9*, No. 2998.
(33) Cifuentes, J. M. C.; Ferreira, B. X.; Esteves, P. M.; Buarque, C. D. Decarboxylative Cross-Coupling of Cinnamic Acids Catalyzed by Iron-Based Covalent Organic Frameworks. *Top. Catal.* **2018**, *61*, 689−698.
(34) Sun, Q.; Fu, C.-W.; Aguila, B.; Perman, J.; Wang, S.; Huang, H.-Y.; Xiao, F.-S.; Ma, S. Pore Environment Control and Enhanced Performance of Enzymes Infiltrated in Covalent Organic Frameworks. *J. Am. Chem. Soc.* **2018**, *140*, 984−992.
(35) Mullangi, D.; Chakraborty, D.; Pradeep, A.; Koshti, V.; Vinod, C. P.; Panja, S.; Nair, S.; Vaidhyanathan, R. Highly Stable COF-Supported Co/$Co(OH)_2$ Nanoparticles Heterogeneous Catalyst for Reduction of Nitrile/Nitro Compounds under Mild Conditions. *Small* **2018**, *14*, No. 1801233.
(36) Sun, Q.; Aguila, B.; Perman, J. A.; Butts, T.; Xiao, F.-S.; Ma, S. Integrating Superwettability within Covalent Organic Frameworks for Functional Coating. *Chem.* **2018**, *4*, 1726−1739.
(37) Shao, P.; Li, J.; Chen, F.; Ma, L.; Li, Q.; Zhang, M.; Zhou, J.; Yin, A.; Feng, X.; Wang, B. Flexible Films of Covalent Organic Frameworks with Ultralow Dielectric Constants under High Humidity. *Angew. Chem., Int. Ed.* **2018**, *57*, 16501−16505.
(38) Gomes, R.; Bhanja, P.; Bhaumik, A. A Triazine-Based Covalent Organic Polymer for Efficient CO_2 Adsorption. *Chem. Commun.* **2015**, *51*, 10050−10053.
(39) Mullangi, D.; Shalini, S.; Nandi, S.; Choksi, B.; Vaidhyanathan, R. Super-Hydrophobic Covalent Organic Frameworks for Chemical Resistant Coatings and Hydrophobic Paper and Textile Composites. *J. Mater. Chem. A* **2017**, *5*, 8376−8384.
(40) Xu, T.; Zhou, L.; He, Y.; An, S.; Peng, C.; Hu, J.; Liu, H. Covalent Organic Framework with Triazine and Hydroxyl Bifunctional Groups for Efficient Removal of Lead(II) Ions. *Ind. Eng. Chem. Res.* **2019**, *58*, 19642−19648.
(41) Mu, M.; Wang, Y.; Qin, Y.; Yan, X.; Li, Y.; Chen, L. Two-Dimensional Imine-Linked Covalent Organic Frameworks as a Platform for Selective Oxidation of Olefins. *ACS Appl. Mater. Interfaces* **2017**, *9*, 22856−22863.
(42) Wulfsberg, G. *Principles of Descriptive Inorganic Chemistry*; University Science Books, 1991; pp 28−30.
(43) Burgess, J. *Metal Ions in Solution*; Ellis Horwood, 1978; p 268.
(44) Alemany, L. B.; Verma, M.; Billups, W. E.; Wellington, S. L.; Shammai, M. Solid- and Solution-State Nuclear Magnetic Resonance Analyses of Ecuadorian Asphaltenes: Quantitative Solid-State Aromaticity Determination Supporting the "Island" Structural Model. Aliphatic Structural Information from Solution-State $^1H-^{13}C$ Heteronuclear Single-Quantum Coherence Experiments. *Energy Fuels* **2015**, *29* (10), 6317−6329.

https://doi.org/10.1021/acs.chemmater.1c00737
Chem. Mater. 2021, 33, 3394−3400